# Supporting Information (SI): Vaccine hesitancy promotes emergence of new SARS-CoV-2 variants

Shuanglin Jing[1,*], Russell Milne[2,*], Hao Wang[2,†], Ling Xue[1]

[1]College of Mathematical Sciences, Harbin Engineering University, Harbin, Heilongjiang, 150001, China

[2]Department of Mathematical and Statistical Sciences & Interdisciplinary Lab for Mathematical Ecology and Epidemiology, University of Alberta, Edmonton, Alberta T6G 2R3, Canada

## Appendix

## A Reproduction number

In this section, we compute the family of disease-free equilibria [1] and the basic reproduction number of Model (4). By setting the left side of the equations in Model (4) to zero, we obtain the family of disease-free equilibria of Model (4) as

$$\begin{aligned}&(S^0, V^0, E^0_{WT}, E^0_{MT}, P^0_{WT}, P^0_{MT}, A^0_{WT}, A^0_{MT}, I^0_{WT}, I^0_{MT}, R^0, x^0)\\&= (N^0 - V^0, V^0, 0, 0, 0, 0, 0, 0, 0, 0, 0, x^0),\end{aligned}$$

where $x^0 \in \{0, 1\}$.

According to the next generation matrix approach presented by van den Driessche and Watmough [2], we obtain the new infection matrix as

$$\mathcal{F} = \begin{pmatrix} 0 & 0 & \frac{\beta_{WT}\theta_{WT}\Phi_1}{N^0} & 0 & \frac{\beta_{WT}\delta_{WT}\Phi_1}{N^0} & 0 & \frac{\beta_{WT}\Phi_1}{N^0} & 0 \\ 0 & 0 & \frac{\beta_{WT}\theta_{WT}\Phi_2}{N^0} & \frac{\beta_{MT}\theta_{MT}\Phi_3}{N^0} & \frac{\beta_{WT}\delta_{WT}\Phi_2}{N^0} & \frac{\beta_{MT}\delta_{MT}\Phi_3}{N^0} & \frac{\beta_{WT}\Phi_2}{N^0} & \frac{\beta_{MT}\Phi_3}{N^0} \\ 0 & 0 & 0 & 0 & 0 & 0 & 0 & 0 \\ 0 & 0 & 0 & 0 & 0 & 0 & 0 & 0 \\ 0 & 0 & 0 & 0 & 0 & 0 & 0 & 0 \\ 0 & 0 & 0 & 0 & 0 & 0 & 0 & 0 \\ 0 & 0 & 0 & 0 & 0 & 0 & 0 & 0 \\ 0 & 0 & 0 & 0 & 0 & 0 & 0 & 0 \end{pmatrix},$$

*These authors contributed equally to this work.

†Corresponding author. E-mail: hao8@ualberta.ca

where $\Phi_1 = (1-u_S)S^0 + (1-u_V)\eta_{WT}V^0$, $\Phi_2 = u_S S^0 + u_V \eta_{WT} V^0$, and $\Phi_3 = S^0 + \eta_{MT}V^0$. The transition matrix and its inverse are

$$\mathcal{V} = \begin{pmatrix} \sigma_{WT} & 0 & 0 & 0 & 0 & 0 & 0 & 0 \\ 0 & \sigma_{MT} & 0 & 0 & 0 & 0 & 0 & 0 \\ -\sigma_{WT} & 0 & \alpha_{WT} & 0 & 0 & 0 & 0 & 0 \\ 0 & -\sigma_{MT} & 0 & \alpha_{MT} & 0 & 0 & 0 & 0 \\ 0 & 0 & -\rho_{WT}\alpha_{WT} & 0 & \gamma_{A_{WT}} & 0 & 0 & 0 \\ 0 & 0 & 0 & -\rho_{MT}\alpha_{MT} & 0 & \gamma_{A_{MT}} & 0 & 0 \\ 0 & 0 & -(1-\rho_{WT})\alpha_{WT} & 0 & 0 & 0 & \gamma_{I_{WT}} & 0 \\ 0 & 0 & 0 & -(1-\rho_{MT})\alpha_{MT} & 0 & 0 & 0 & \gamma_{I_{MT}} \end{pmatrix},$$

and

$$\mathcal{V}^{-1} = \begin{pmatrix} \frac{1}{\sigma_{WT}} & 0 & 0 & 0 & 0 & 0 & 0 & 0 \\ 0 & \frac{1}{\sigma_{MT}} & 0 & 0 & 0 & 0 & 0 & 0 \\ \frac{1}{\alpha_{WT}} & 0 & \frac{1}{\alpha_{WT}} & 0 & 0 & 0 & 0 & 0 \\ 0 & \frac{1}{\alpha_{MT}} & 0 & \frac{1}{\alpha_{MT}} & 0 & 0 & 0 & 0 \\ \frac{\rho_{WT}}{\gamma_{A_{WT}}} & 0 & \frac{\rho_{WT}}{\gamma_{A_{WT}}} & 0 & \frac{1}{\gamma_{A_{WT}}} & 0 & 0 & 0 \\ 0 & \frac{\rho_{MT}}{\gamma_{A_{MT}}} & 0 & \frac{\rho_{MT}}{\gamma_{A_{MT}}} & 0 & \frac{1}{\gamma_{A_{MT}}} & 0 & 0 \\ \frac{1-\rho_{WT}}{\gamma_{I_{WT}}} & 0 & \frac{1-\rho_{WT}}{\gamma_{I_{WT}}} & 0 & 0 & 0 & \frac{1}{\gamma_{I_{WT}}} & 0 \\ 0 & \frac{1-\rho_{MT}}{\gamma_{I_{MT}}} & 0 & \frac{1-\rho_{MT}}{\gamma_{I_{MT}}} & 0 & 0 & 0 & \frac{1}{\gamma_{I_{MT}}} \end{pmatrix},$$

respectively. The basic reproduction number $R_0$, i.e. the spectral radius of the matrix product $\mathcal{F}\mathcal{V}^{-1}$, is

$$R_0 = \max\left\{R_0^{WT}, R_0^{MT}\right\}, \tag{A.1}$$

where the basic reproduction number for WT is

$$R_0^{WT} = \frac{(1-u_S)S^0 + (1-u_V)\eta_{WT}V^0}{N^0}\left(\frac{\beta_{WT}\theta_{WT}}{\alpha_{WT}} + \frac{\beta_{WT}\rho_{WT}\delta_{WT}}{\gamma_{A_{WT}}} + \frac{\beta_{WT}(1-\rho_{WT})}{\gamma_{I_{WT}}}\right), \tag{A.2}$$

and that for MT is

$$R_0^{MT} = \frac{S^0 + \eta_{MT}V^0}{N^0}\left(\frac{\beta_{MT}\theta_{MT}}{\alpha_{MT}} + \frac{\beta_{MT}\rho_{MT}\delta_{MT}}{\gamma_{A_{MT}}} + \frac{\beta_{MT}(1-\rho_{MT})}{\gamma_{I_{MT}}}\right). \tag{A.3}$$

In the above equations for the basic reproduction numbers of the two SARS-CoV-2 strains, the three terms within the parentheses represent the daily numbers of new cases generated by pre-symptomatic, asymptomatic, and symptomatic individuals, respectively. While transmission potential at the beginning of an epidemic is often measured using the basic reproduction number [3], this potential varies as an outbreak progresses. We therefore additionally define the effective reproduction number, which measures transmission potential at any point during a given outbreak. As with the basic reproduction number, the effective reproduction number in this model is also defined as the maximum of that of WT and that of MT, specifically as

$$R_e(t) = \max\left\{R_e^{WT}(t), R_e^{MT}(t)\right\}, \tag{A.4}$$

where

$$\begin{aligned}
R_e^{WT}(t) &= \frac{(1-u_S)S(t) + (1-u_V)\eta_{WT}V(t)}{N(t)}\left(\frac{\beta_{WT}\theta_{WT}}{\alpha_{WT}} + \frac{\beta_{WT}\rho_{WT}\delta_{WT}}{\gamma_{A_{WT}}} + \frac{\beta_{WT}(1-\rho_{WT})}{\gamma_{I_{WT}}}\right),\\
R_e^{MT}(t) &= \frac{S(t) + \eta_{MT}V(t)}{N(t)}\left(\frac{\beta_{MT}\theta_{MT}}{\alpha_{MT}} + \frac{\beta_{MT}\rho_{MT}\delta_{MT}}{\gamma_{A_{MT}}} + \frac{\beta_{MT}(1-\rho_{MT})}{\gamma_{I_{MT}}}\right).
\end{aligned}$$

# B Semi-stochastic simulation

As part of our work on evaluating the probability of mutant SARS-CoV-2 strains emerging, we performed semi-stochastic simulations featuring the state variables in Model 4 in the main text. To do this, we first described 32 events that represent individuals moving between the states within Model 4, and then assigned time-varying probabilities to them. The events and their associated probabilities are listed in Table 1. The total rate at which any one of these possible events occurs can be expressed as

$$\begin{aligned}
T_{all}(t) =& \frac{(1-u_S)\beta_{WT}(\theta_{WT}P_{WT}(t) + \delta_{WT}A_{WT}(t) + I_{WT}(t))S(t)}{N(t)}\\
&+ \frac{u_S\beta_{WT}(\theta_{WT}P_{WT}(t) + \delta_{WT}A_{WT}(t) + I_{WT}(t))S(t)}{N(t)}\\
&+ \frac{\beta_{MT}(\theta_{MT}P_{MT}(t) + \delta_{MT}A_{MT}(t) + I_{MT}(t))S(t)}{N(t)}\\
&+ \frac{(1-u_S)\beta_{WT}(\theta_{WT}P_{WT}(t) + \delta_{WT}A_{WT}(t) + I_{WT}(t))\eta_{WT}V(t)}{N(t)}\\
&+ \frac{u_S\beta_{WT}(\theta_{WT}P_{WT}(t) + \delta_{WT}A_{WT}(t) + I_{WT}(t))\eta_{WT}V(t)}{N(t)}\\
&+ \frac{\beta_{MT}(\theta_{MT}P_{MT}(t) + \delta_{MT}A_{MT}(t) + I_{MT}(t))\eta_{MT}V(t)}{N(t)}\\
&+ px(t)S(t) + \tau V(t) + \sum_{i=\{WT,MT\}}\Big[\sigma_i E_i(t) + \rho_i\alpha_i P_i(t)\\
&+ (1-\rho_i)\alpha_i P_i(t) + \gamma_{A_i}A_i(t) + \mu_i\gamma_{I_i}I_i(t) + (1-\mu_i)\gamma_{I_i}I_i(t)\Big],
\end{aligned} \tag{B.5}$$

where $x(t)$ is the solution of the differential equation

$$\frac{\mathrm{d}x}{\mathrm{d}t} = kx(1-x)\Delta F.$$

In order to ensure consistency across model runs, we used a fixed time step $\mathrm{d}t$ such that $T_{all}(t)\mathrm{d}t \leq 1$. At each point in time during a simulation, we divided the $[0, 1]$ interval into 33 smaller intervals, that is,

$$\left[0,\ T_1\mathrm{d}t\right], \left[T_1\mathrm{d}t,\ \sum_{i=1}^{2} T_i\mathrm{d}t\right], \left[\sum_{i=1}^{2} T_i\mathrm{d}t,\ \sum_{i=1}^{3} T_i\mathrm{d}t\right], \ldots,$$
$$\left[\sum_{i=1}^{j-1} T_i\mathrm{d}t,\ \sum_{i=1}^{j} T_i\mathrm{d}t\right], \ldots, \left[\sum_{i=1}^{31} T_i\mathrm{d}t,\ \sum_{i=1}^{32} T_i\mathrm{d}t\right], \left[T_{all}\mathrm{d}t,\ 1\right].$$

Note that $T_{all}\mathrm{d}t = \sum_{i=1}^{32} T_i\mathrm{d}t$, as can be seen in Equation (B.5) and Table 1. Next, we choose a constant $U$, where $U$ is a uniform random variable within $[0, 1]$. If $U \in \left[\sum_{i=1}^{j-1} T_i\mathrm{d}t,\ \sum_{i=1}^{j} T_i\mathrm{d}t\right]$, then event $T_j$ occurs, whereas if $U \in \left[T_{all}\mathrm{d}t,\ 1\right]$, no event occurs. In the following we provide illustrative examples, using events that involve symptomatic individuals infected with WT ($I_{WT}(t)$ in our model). In each infinitesimally small time step $\mathrm{d}t$, there is a probability $\beta_{WT} I_{WT}(t)S(t)\mathrm{d}t/N$ that a symptomatic individual carrying WT comes in contact with a susceptible individual and causes them to become exposed to SARS-CoV-2.

Within this event, if the mutation occurs, the number of susceptible individuals is decreased by 1 (i.e. $S(t) \to S(t) - 1$), the number of exposed individuals infected with the mutant strain of SARS-CoV-2 $E_{MT}(t)$ grows by 1 (i.e. $E_{MT}(t) \to E_{MT}(t) + 1$). Otherwise, the number of susceptible individuals is decreased by 1 (i.e. $S(t) \to S(t) - 1$), the number of exposed individuals infected with WT $E_{WT}(t)$ grows by 1 (i.e. $E_{WT}(t) \to E_{WT}(t) + 1$). Similarly, symptomatic individuals infected with WT are removed with probability $\gamma_{I_{WT}} I_{WT}(t)\mathrm{d}t$. During this event, when the infected individual recovers, $I_{WT}(t)$ is decreased by 1 (i.e. $I_{WT}(t) \to I_{WT}(t) - 1$), while the numbers of recovered individuals are increased by 1 (i.e. $R(t) \to R(t) + 1$). When the infected individual die, $I_{WT}(t)$ is decreased by 1 (i.e. $I_{WT}(t) \to I_{WT}(t) - 1$), while the numbers of dead individuals are increased by 1 (i.e. $D(t) \to D(t) + 1$).

# C Additional figures

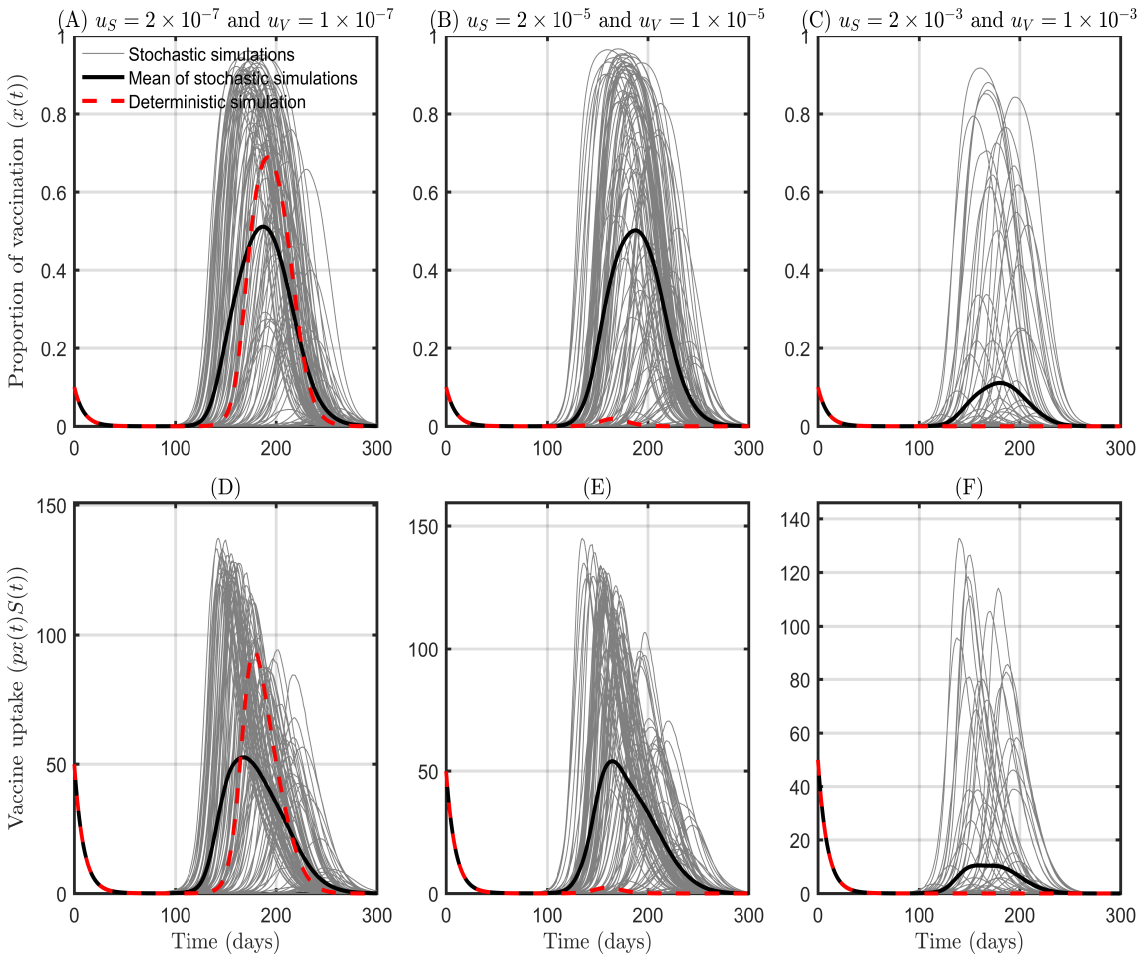


Figure C.1: The effect of mutation probability ($u_S$ and $u_V$) on the proportion of vaccination and vaccine uptake. The results of deterministic and 100 stochastic simulations of time series of proportion of vaccination when mutation probability is $u_S = 2 \times 10^{-7}$ and $u_V = 1 \times 10^{-7}$; $u_S = 2 \times 10^{-5}$ and $u_V = 1 \times 10^{-5}$; and $u_S = 2 \times 10^{-3}$ and $u_V = 1 \times 10^{-3}$ are shown in Subfigures A, B, and C, respectively. Subfigures D, E, and F show the change of vaccine uptake over time, for the same values of $u_S$ and $u_V$ in the order specified above. Values of other parameters are $r_v = 0.6$, $r_{A_{WT}} = 0.05$, and $r_{I_{WT}} = 0.06$.

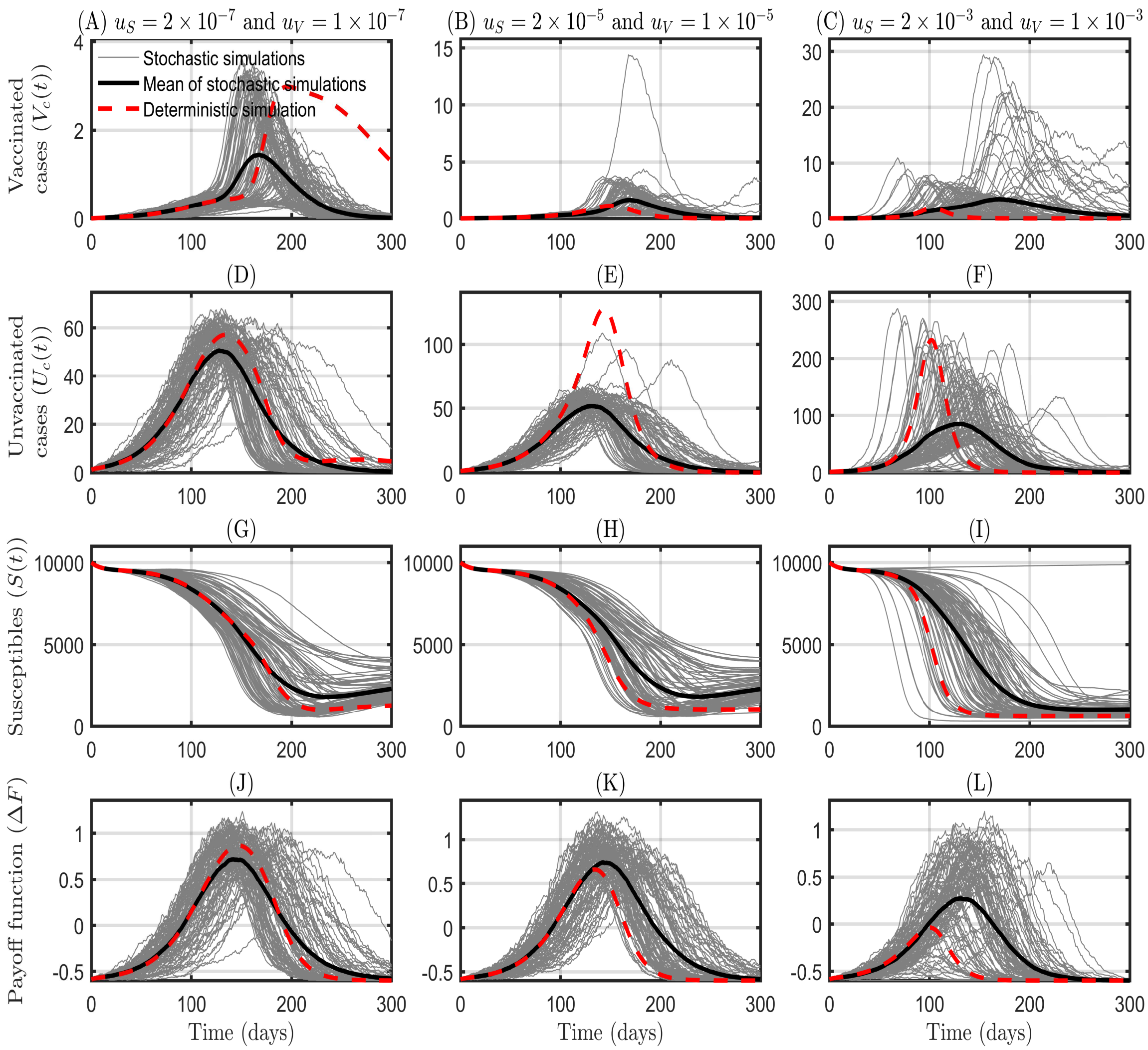


Figure C.2: The effect of mutation probability ($u_S$ and $u_V$) on the vaccinated cases, unvaccinated cases, susceptibles, and payoff function. The results of deterministic and 100 stochastic simulations of time series of vaccinated (unvaccinated) cases when mutation probability is $u_S = 2 \times 10^{-7}$ and $u_V = 1 \times 10^{-7}$; $u_S = 2 \times 10^{-5}$ and $u_V = 1 \times 10^{-5}$; and $u_S = 2 \times 10^{-3}$ and $u_V = 1 \times 10^{-3}$ are shown in Subfigures A, B, and C (D, E, and F), respectively. Subfigures G, H, I, J, K, and L show the changes of susceptibles and payoff function over time, for the same values of $u_S$ and $u_V$ in the order specified above. Values of other parameters are $r_v = 0.6$, $r_{A_{WT}} = 0.05$, and $r_{I_{WT}} = 0.06$.

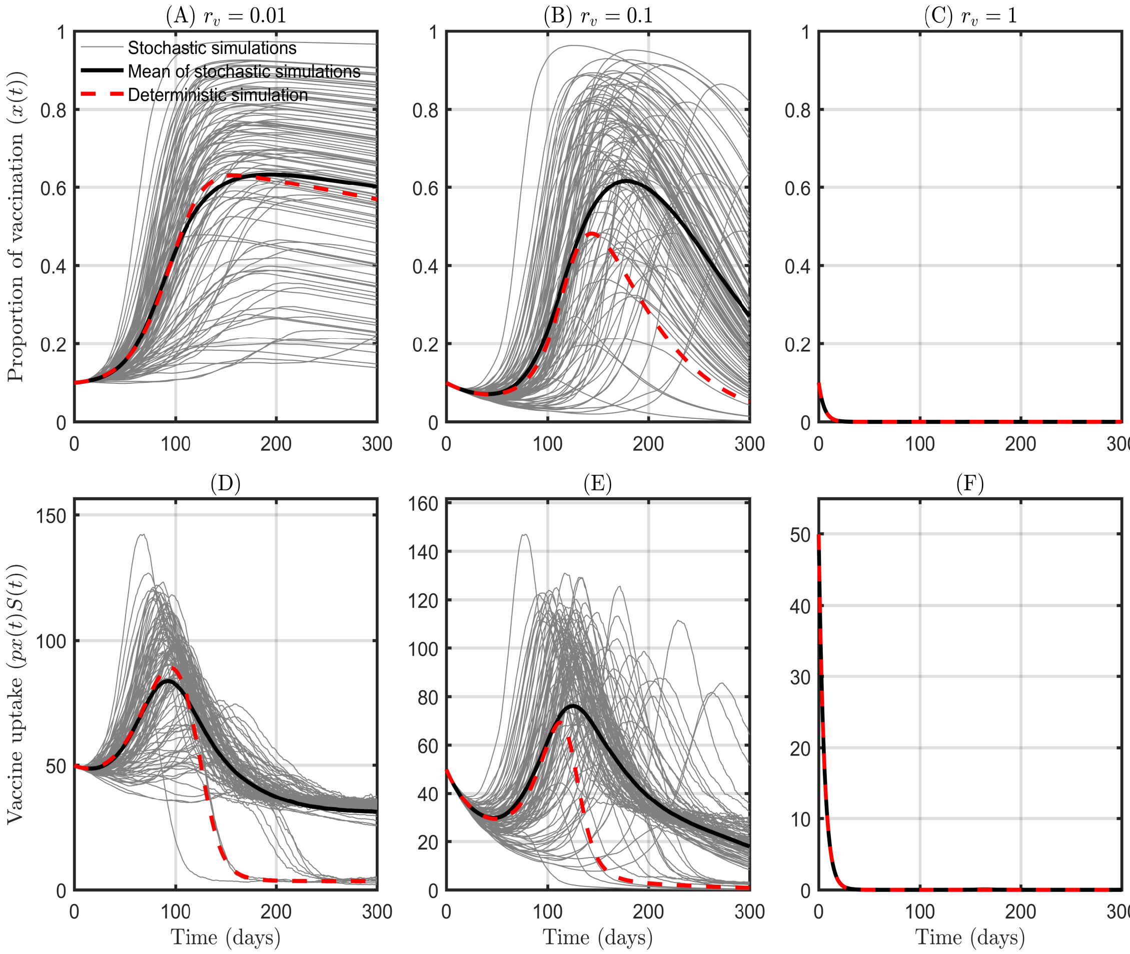


Figure C.3: The effect of perceived costs of vaccinators ($r_v$) on the proportion of vaccination and vaccine uptake. The results of deterministic and 100 stochastic simulations of time series of proportion of vaccination when perceived costs of vaccinators are $r_v = 0.01$, $r_v = 0.1$, and $r_v = 1$ are shown in Subfigures A, B, and C, respectively. Subfigures D, E, and F show the change of vaccine uptake over time, for the same values of $r_v$ in the order specified above. Values of other parameters are $u_S = 2 \times 10^{-4}$, $u_V = 1 \times 10^{-4}$, $r_{A_{WT}} = 0.05$, and $r_{I_{WT}} = 0.06$.

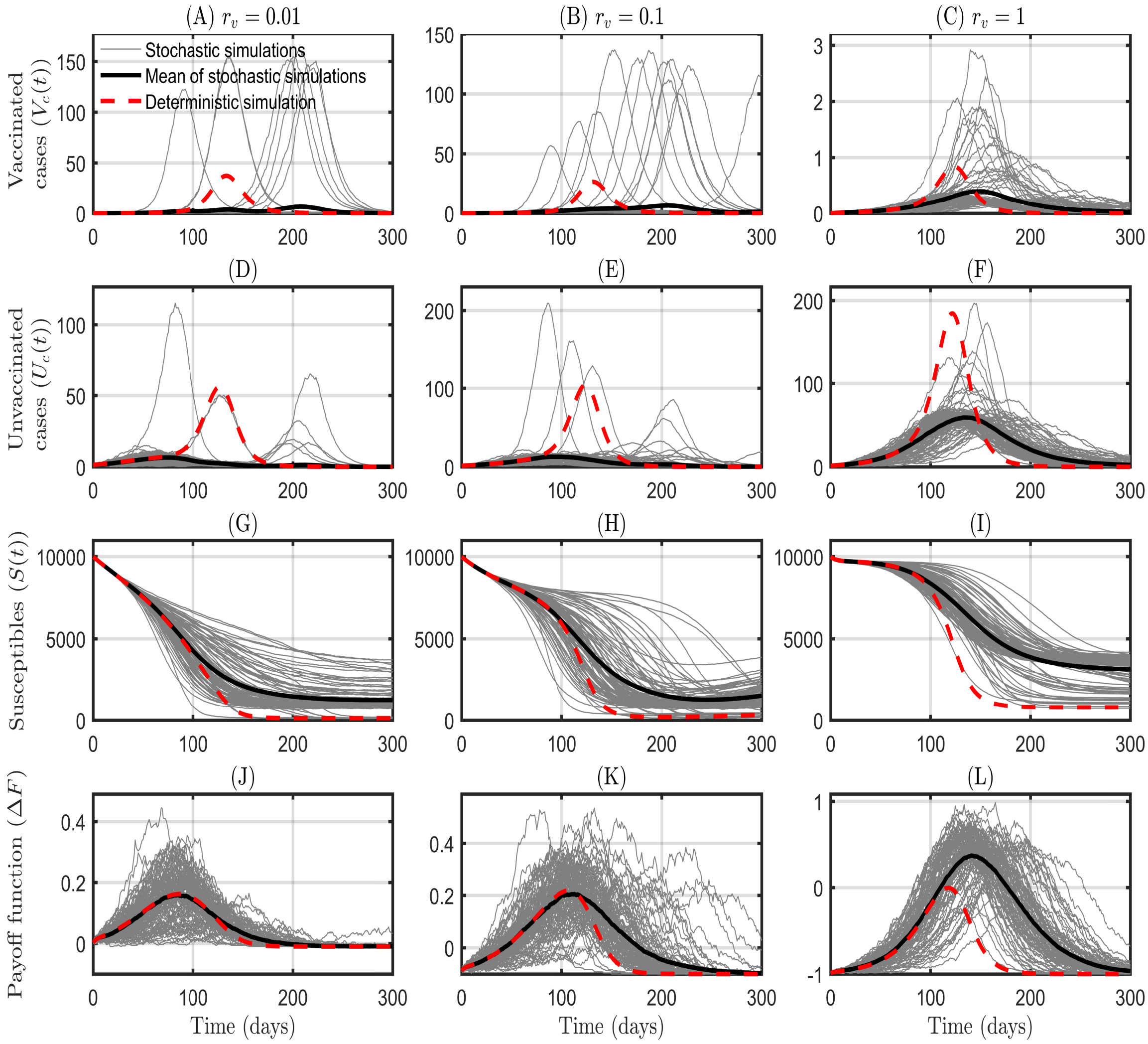


Figure C.4: The effect of perceived costs of vaccinators ($r_v$) on the vaccinated cases, unvaccinated cases, susceptibles, and payoff function. The results of deterministic and 100 stochastic simulations of time series of vaccinated (unvaccinated) cases when perceived costs of vaccinators are $r_v = 0.01$, $r_v = 0.1$, and $r_v = 1$ are shown in Subfigures A, B, and C (D, E, and F), respectively. Subfigures G, H, I, J, K, and L show the changes of susceptibles and payoff function over time, for the same values of $r_v$ in the order specified above. Values of other parameters are $u_S = 2 \times 10^{-4}$, $u_V = 1 \times 10^{-4}$, $r_{A_{WT}} = 0.05$, and $r_{I_{WT}} = 0.06$.

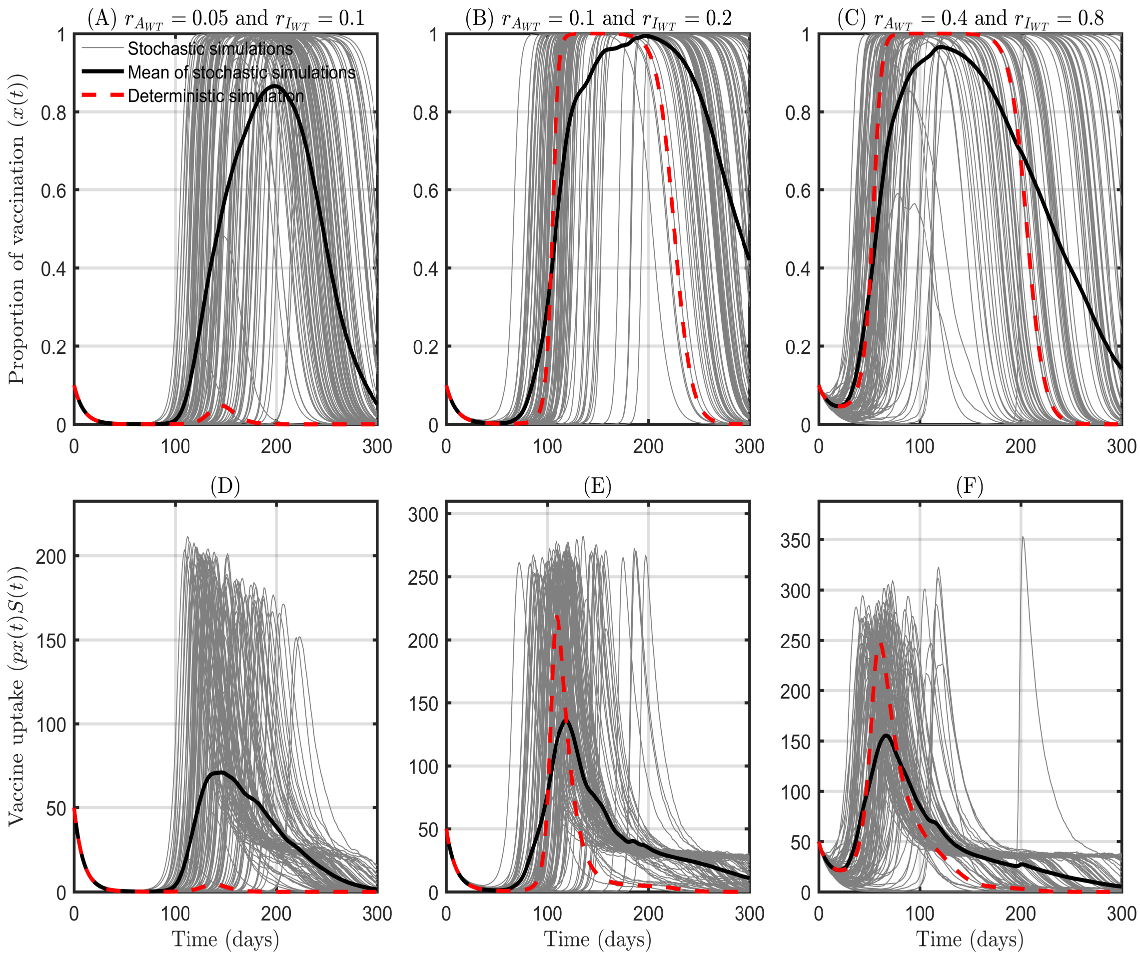


Figure C.5: The effect of perceived risks of WT infection ($r_{A_{WT}}$ and $r_{I_{WT}}$) on the proportion of vaccination and vaccine uptake. The results of deterministic and 100 stochastic simulations of time series of proportion of vaccination when perceived risks of infection are $r_{A_{WT}} = 0.05$ and $r_{I_{WT}} = 0.1$; $r_{A_{WT}} = 0.1$ and $r_{I_{WT}} = 0.2$; and $r_{A_{WT}} = 0.4$ and $r_{I_{WT}} = 0.8$ are shown in Subfigures A, B, and C, respectively. Subfigures D, E, and F show the change of vaccine uptake over time, for the same sets of values of $r_{A_{WT}}$ and $r_{I_{WT}}$, in the order specified above. Values of other parameters are $u_S = 2 \times 10^{-4}$, $u_V = 1 \times 10^{-4}$, and $r_v = 0.6$.

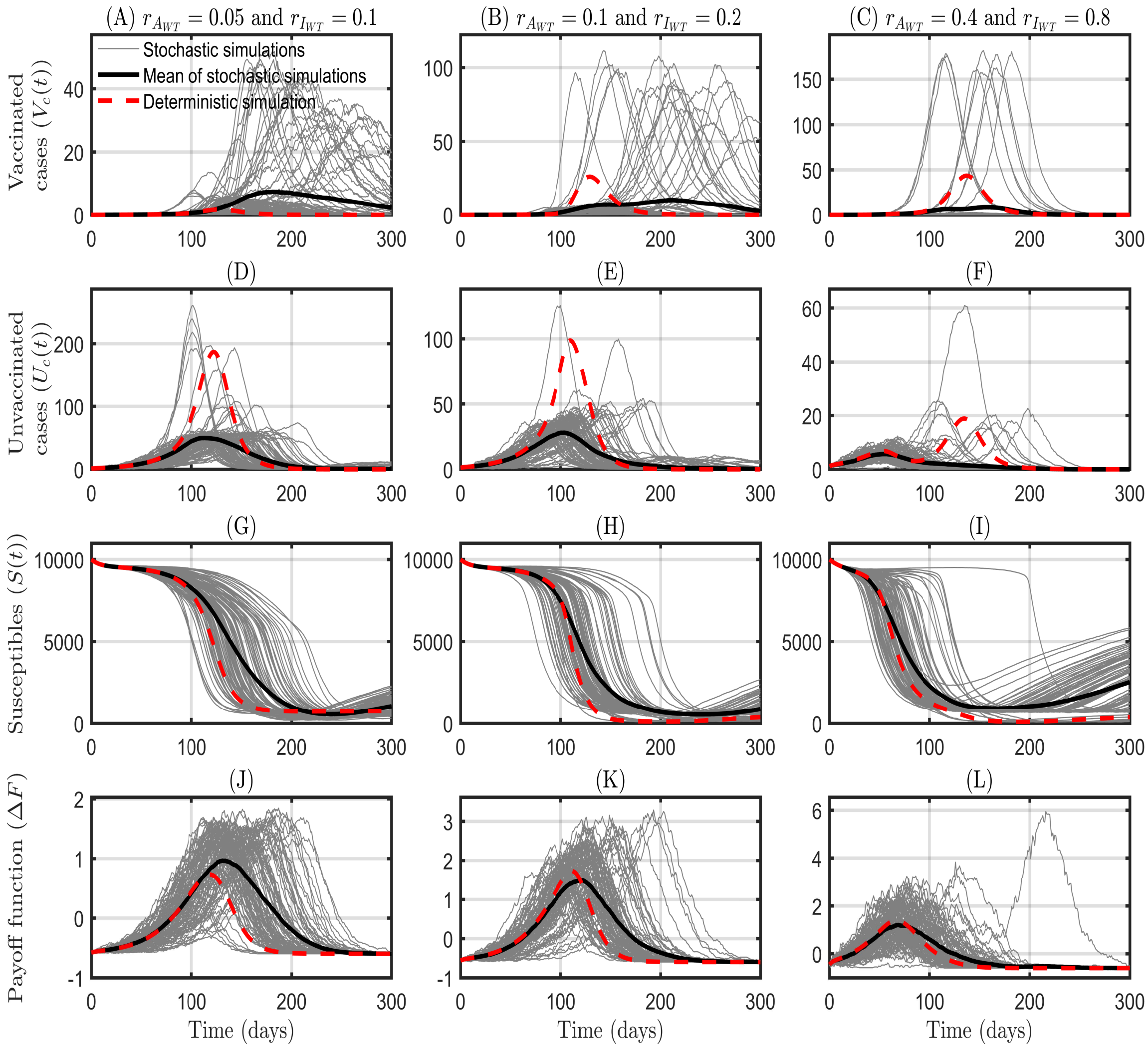


Figure C.6: The effect of perceived risks of WT infection ($r_{A_{WT}}$ and $r_{I_{WT}}$) on the vaccinated cases, unvaccinated cases, susceptibles, and payoff function. The results of deterministic and 100 stochastic simulations of time series of vaccinated (unvaccinated) cases when perceived risks of infection are $r_{A_{WT}} = 0.05$ and $r_{I_{WT}} = 0.1$; $r_{A_{WT}} = 0.1$ and $r_{I_{WT}} = 0.2$; and $r_{A_{WT}} = 0.4$ and $r_{I_{WT}} = 0.8$ are shown in Subfigures A, B, and C (D, E, and F), respectively. Subfigures G, H, I, J, K, and L show the changes of susceptibles and payoff function over time, for the same sets of values of $r_{A_{WT}}$ and $r_{I_{WT}}$, in the order specified above. Values of other parameters are $u_S = 2 \times 10^{-4}$, $u_V = 1 \times 10^{-4}$, and $r_v = 0.6$.

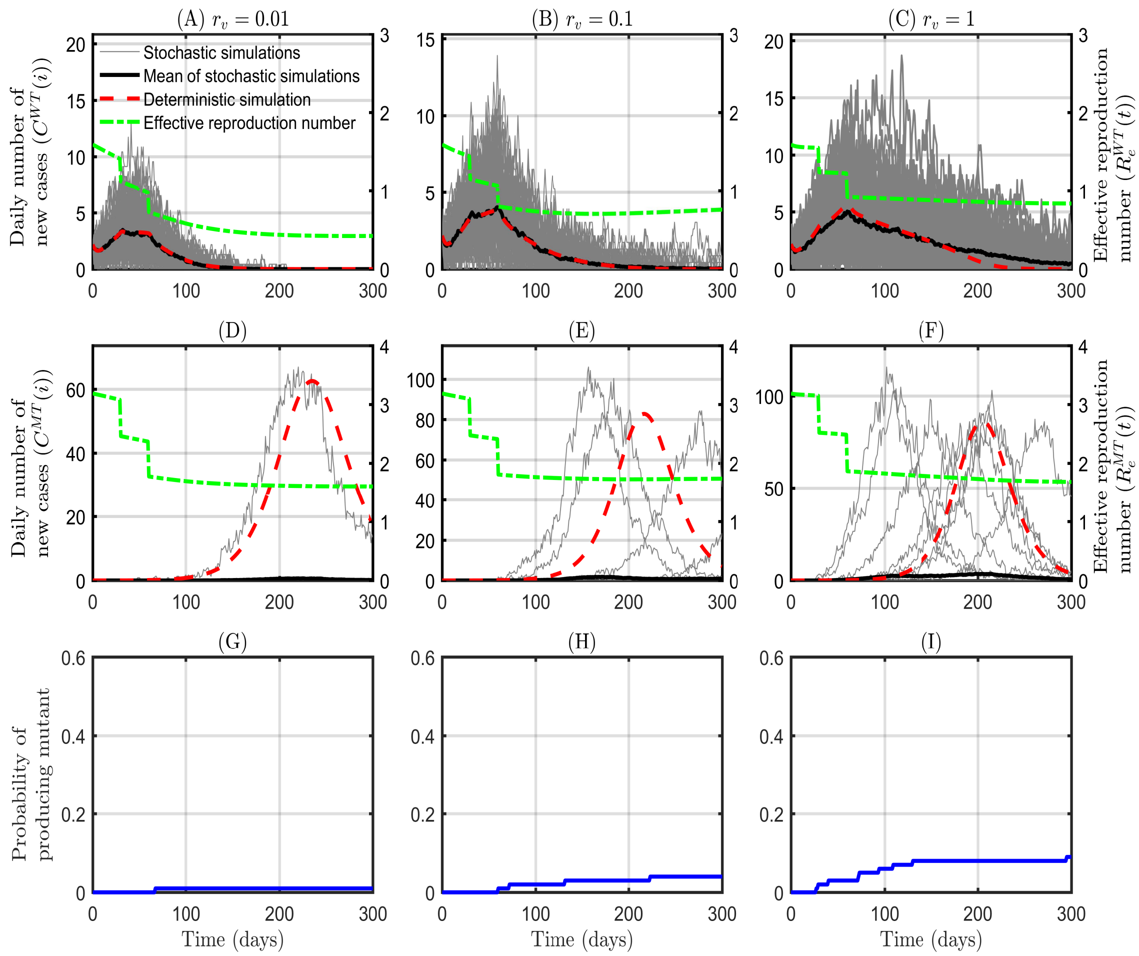


Figure C.7: The effect of perceived costs of vaccinators ($r_v$) on the probability of emergence of MT under non-pharmaceutical interventions with moderately high mutation rates. Subfigures A, B, and C (D, E, and F) show the results of deterministic and 100 stochastic simulations and the effective reproduction number of WT (MT), i.e. $R_e^{WT}(t)$ ($R_e^{MT}(t)$), when perceived costs of vaccinators are $r_v = 0.01$, $r_v = 0.1$, and $r_v = 1$, respectively. Subfigures G, H, and I show the probability of producing a mutant strain over time, for the same values of $r_v$ in the order specified above. Values of other parameters are $u_S = 2 \times 10^{-4}$, $u_V = 1 \times 10^{-4}$, $r_{A_{WT}} = 0.05$, and $r_{I_{WT}} = 0.06$.

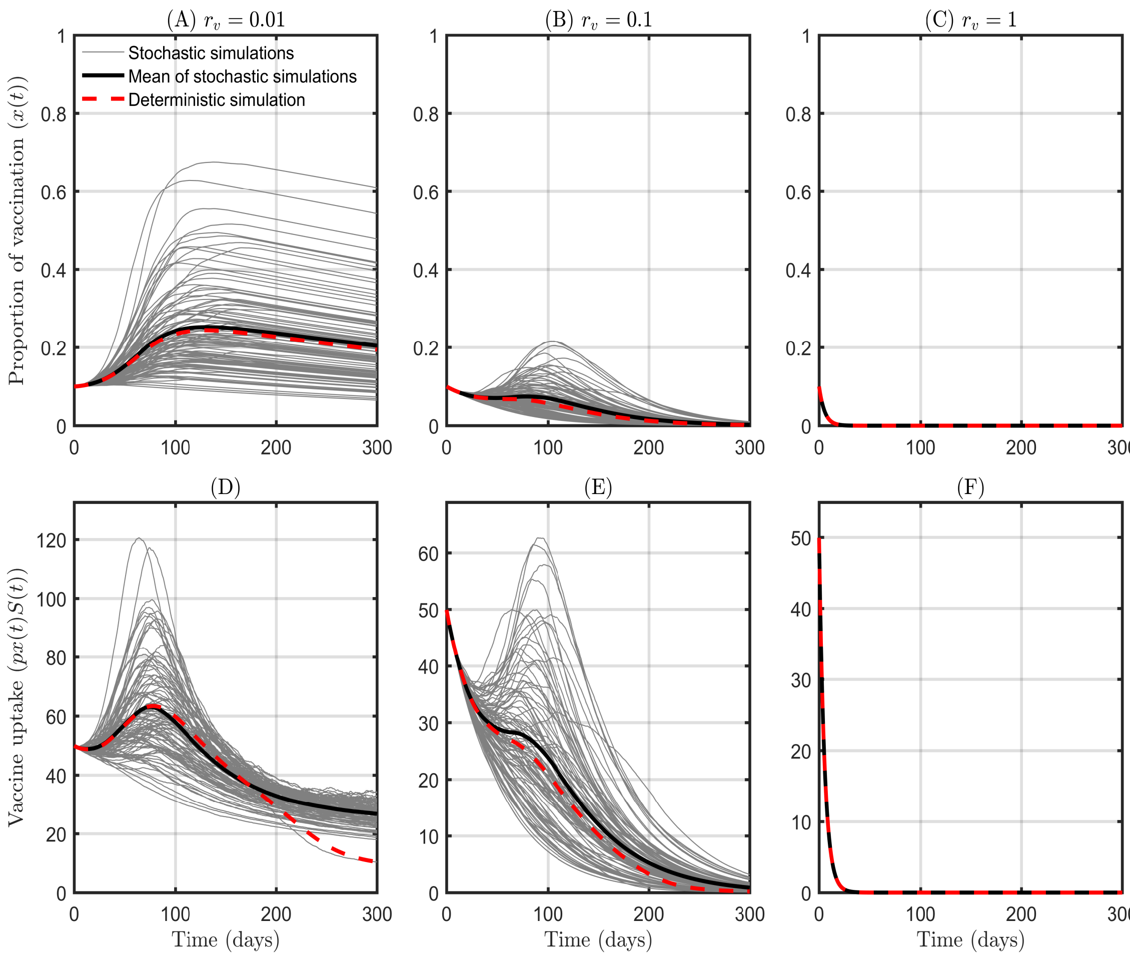


Figure C.8: The effect of perceived costs of vaccinators ($r_v$) on the proportion of vaccination and vaccine uptake under non-pharmaceutical interventions with moderately high mutation rates. Subfigures A, B, and C show the results of deterministic and 100 stochastic simulations of proportion of vaccination, when perceived costs of vaccinators are $r_v = 0.01$, $r_v = 0.1$, and $r_v = 1$, respectively. Subfigures D, E, and F show the change of vaccine uptake over time, for the same values of $r_v$ in the order specified above. Values of other parameters are $u_S = 2 \times 10^{-4}$, $u_V = 1 \times 10^{-4}$, $r_{A_{WT}} = 0.05$, and $r_{I_{WT}} = 0.06$.

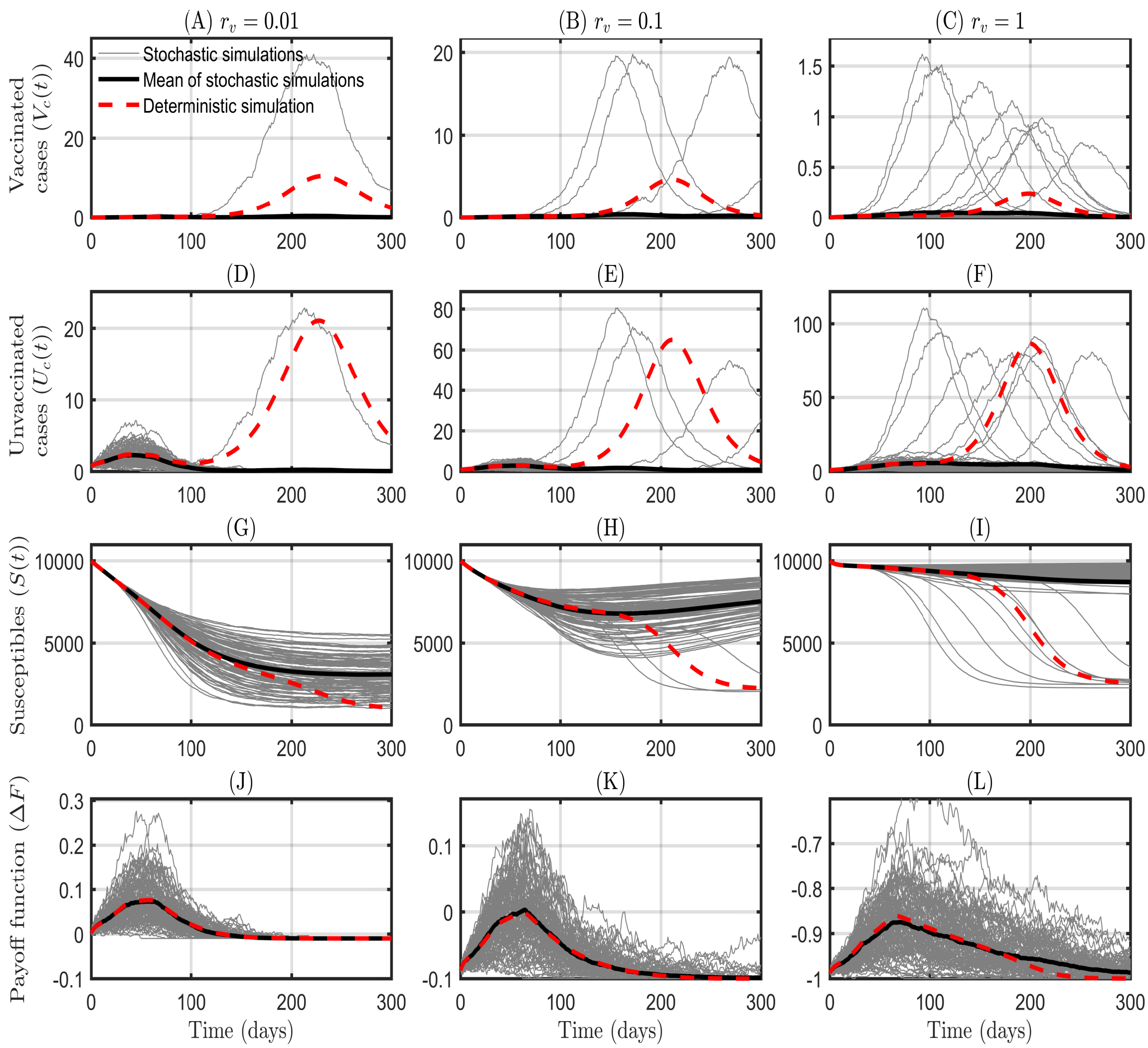


Figure C.9: The effect of perceived costs of vaccinators ($r_v$) on the vaccinated cases, unvaccinated cases, susceptibles, and payoff function under non-pharmaceutical interventions with moderately high mutation rates. Subfigures A, B, and C (D, E, and F) show the results of deterministic and 100 stochastic simulations of vaccinated (unvaccinated) cases, when perceived costs of vaccinators are $r_v = 0.01$, $r_v = 0.1$, and $r_v = 1$, respectively. Subfigures G, H, I, J, K, and L show the changes of susceptibles and payoff function over time, for the same values of $r_v$ in the order specified above. Values of other parameters are $u_S = 2 \times 10^{-4}$, $u_V = 1 \times 10^{-4}$, $r_{A_{WT}} = 0.05$, and $r_{I_{WT}} = 0.06$.

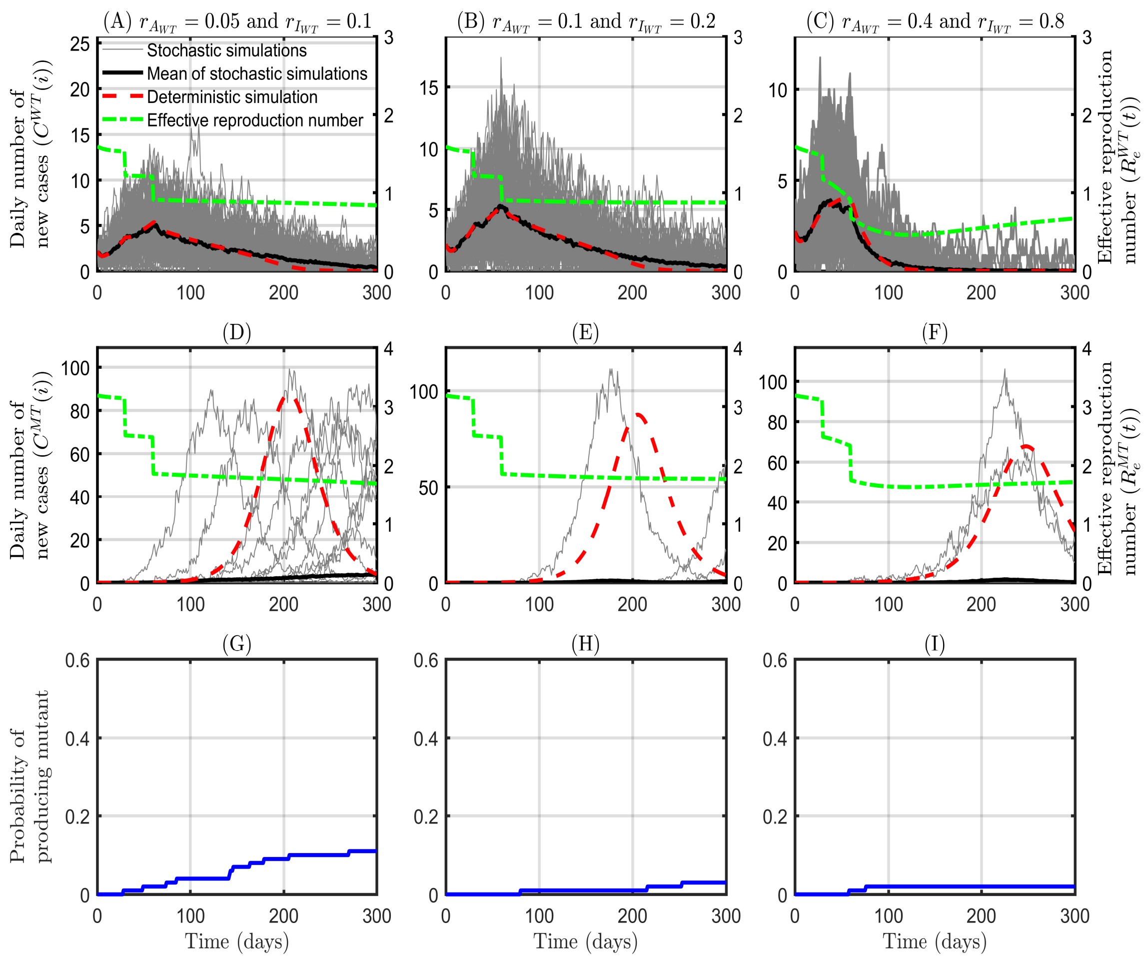


Figure C.10: The effect of perceived risks of WT infection ($r_{A_{WT}}$ and $r_{I_{WT}}$) on the probability of emergence of MT under non-pharmaceutical interventions with moderately high mutation rates. Subfigures A, B, and C (D, E, and F) show the results of deterministic and 100 stochastic simulations and the effective reproduction number of WT (MT), i.e. $R_e^{WT}(t)$ ($R_e^{MT}(t)$), when perceived risks of infection are $r_{A_{WT}} = 0.05$ and $r_{I_{WT}} = 0.1$; $r_{A_{WT}} = 0.1$ and $r_{I_{WT}} = 0.2$; and $r_{A_{WT}} = 0.4$ and $r_{I_{WT}} = 0.8$, respectively. Subfigures G, H, and I show the probability of producing a mutant strain over time, for the same sets of values of $r_{A_{WT}}$ and $r_{I_{WT}}$, in the order specified above. Values of other parameters are $u_S = 2 \times 10^{-4}$, $u_V = 1 \times 10^{-4}$, and $r_v = 0.6$.

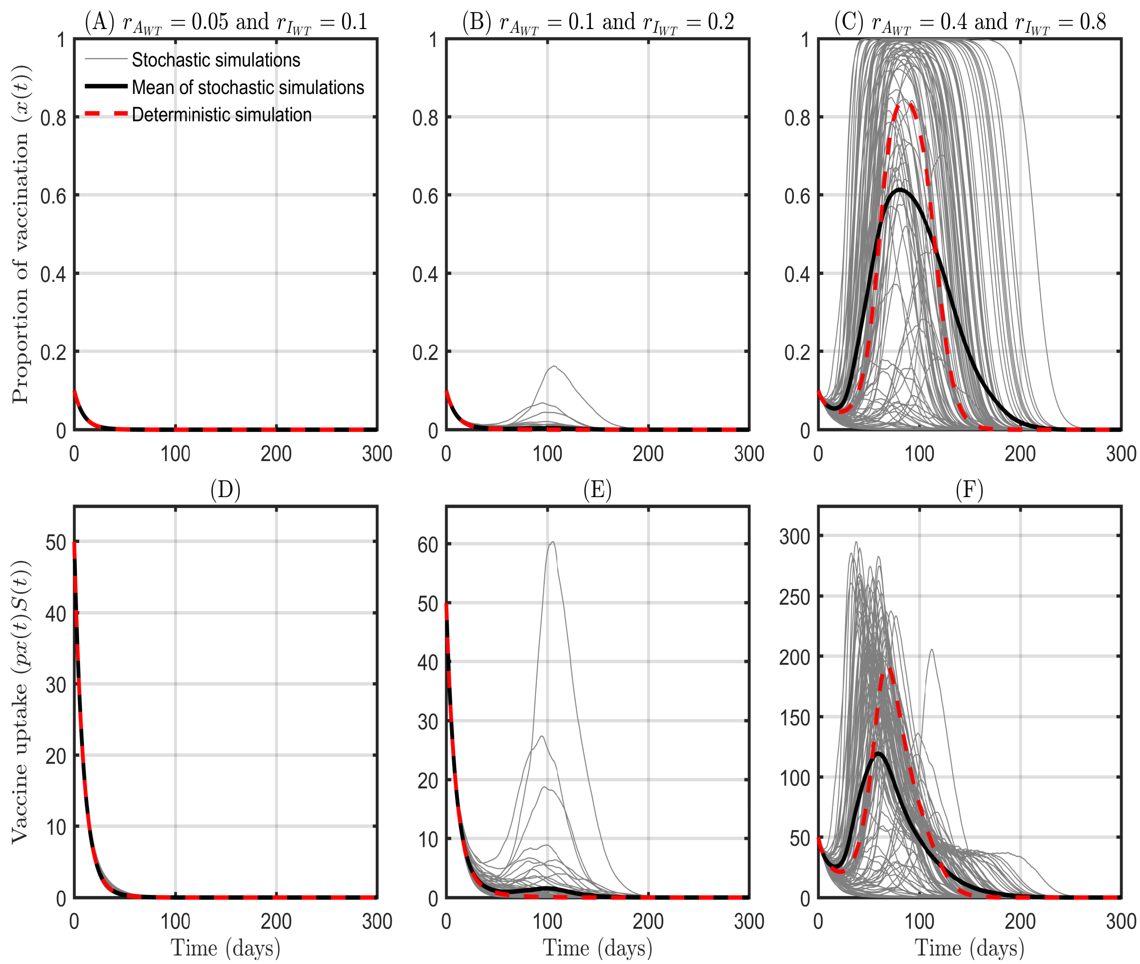


Figure C.11: The effect of perceived risks of WT infection ($r_{A_{WT}}$ and $r_{I_{WT}}$) on the proportion of vaccination and vaccine uptake under non-pharmaceutical interventions with moderately high mutation rates. Subfigures A, B, and C show the results of deterministic and 100 stochastic simulations of proportion of vaccination, when perceived risks of infection are $r_{A_{WT}} = 0.05$ and $r_{I_{WT}} = 0.1$; $r_{A_{WT}} = 0.1$ and $r_{I_{WT}} = 0.2$; and $r_{A_{WT}} = 0.4$ and $r_{I_{WT}} = 0.8$, respectively. Subfigures D, E, and F show the change of vaccine uptake over time, for the same sets of values of $r_{A_{WT}}$ and $r_{I_{WT}}$, in the order specified above. Values of other parameters are $u_S = 2 \times 10^{-4}$, $u_V = 1 \times 10^{-4}$, and $r_v = 0.6$.

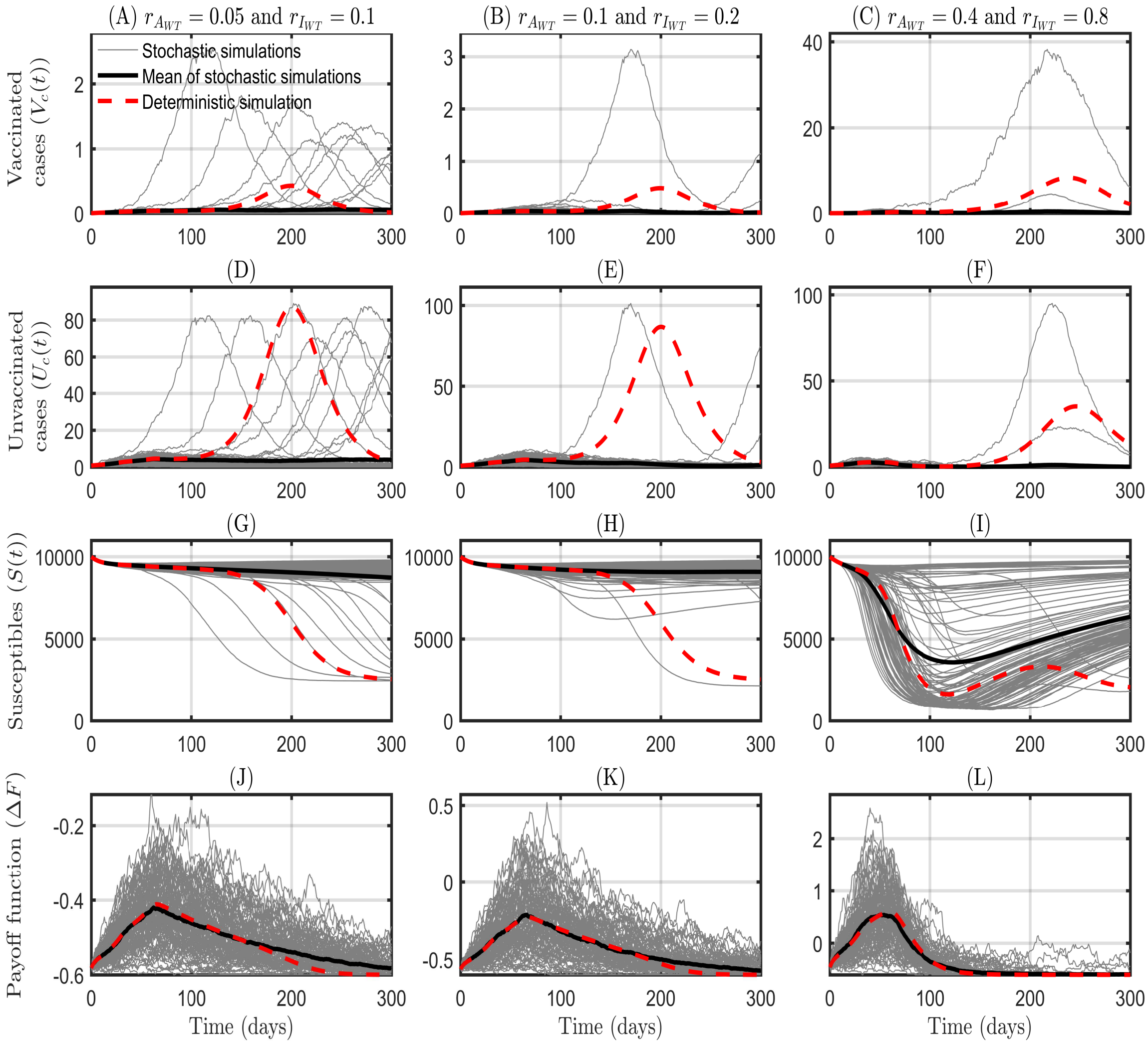


Figure C.12: The effect of perceived risks of WT infection ($r_{A_{WT}}$ and $r_{I_{WT}}$) on the vaccinated cases, unvaccinated cases, susceptibles, and payoff function under non-pharmaceutical interventions with moderately high mutation rates. Subfigures A, B, and C (D, E, and F) show the results of deterministic and 100 stochastic simulations of vaccinated (unvaccinated) cases, when perceived risks of infection are $r_{A_{WT}} = 0.05$ and $r_{I_{WT}} = 0.1$; $r_{A_{WT}} = 0.1$ and $r_{I_{WT}} = 0.2$; and $r_{A_{WT}} = 0.4$ and $r_{I_{WT}} = 0.8$, respectively. Subfigures G, H, I, J, K, and L show the changes of susceptibles and payoff function over time, for the same sets of values of $r_{A_{WT}}$ and $r_{I_{WT}}$, in the order specified above. Values of other parameters are $u_S = 2 \times 10^{-4}$, $u_V = 1 \times 10^{-4}$, and $r_v = 0.6$.

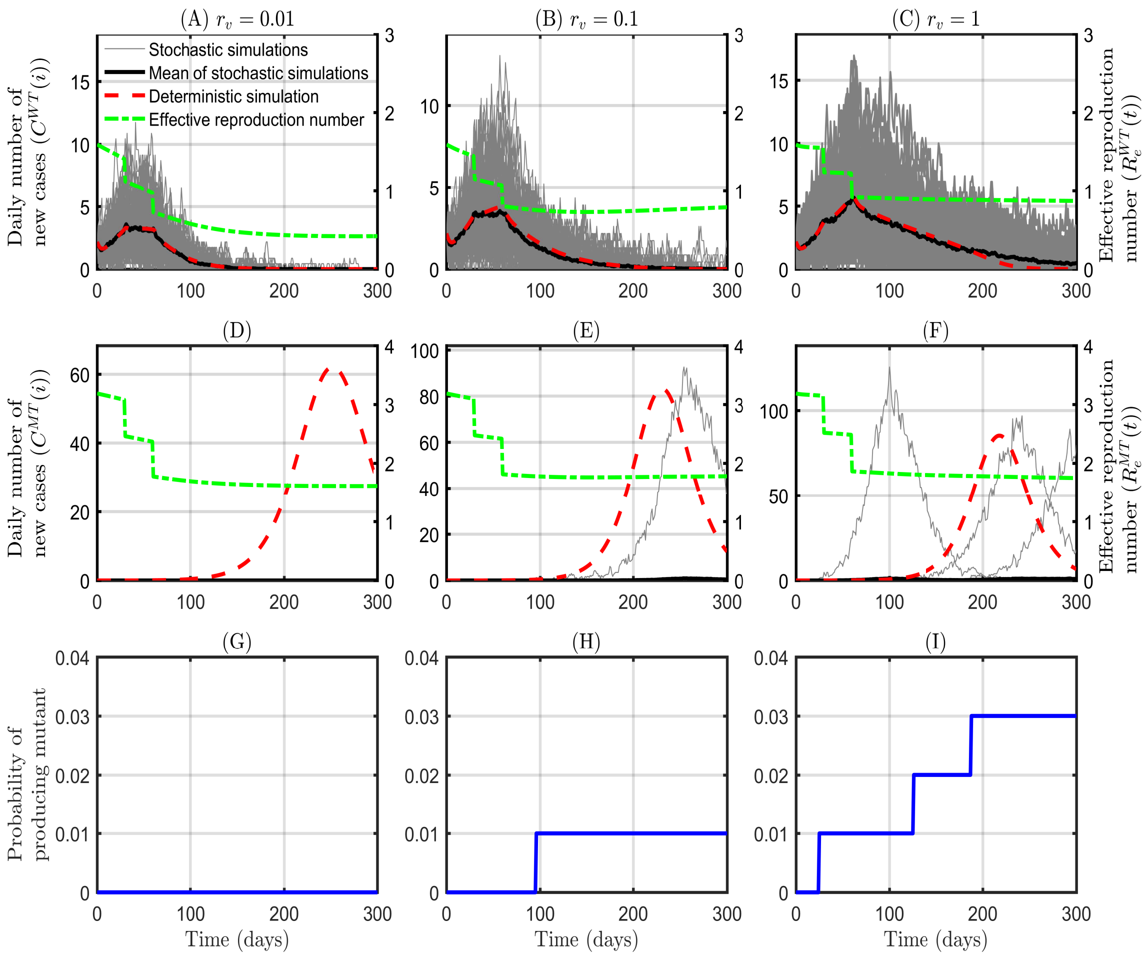


Figure C.13: The effect of perceived costs of vaccinators ($r_v$) on the probability of emergence of MT under non-pharmaceutical interventions with moderately low mutation rates. Subfigures A, B, and C (D, E, and F) show the results of deterministic and 100 stochastic simulations and the effective reproduction number of WT (MT), i.e. $R_e^{WT}(t)$ ($R_e^{MT}(t)$), when perceived costs of vaccinators are $r_v = 0.01$, $r_v = 0.1$, and $r_v = 1$, respectively. Subfigures G, H, and I show the probability of producing a mutant strain over time, for the same values of $r_v$ in the order specified above. Values of other parameters are $u_S = 1 \times 10^{-4}$, $u = 5 \times 10^{-5}$, $r_{A_{WT}} = 0.05$, and $r_{I_{WT}} = 0.06$.

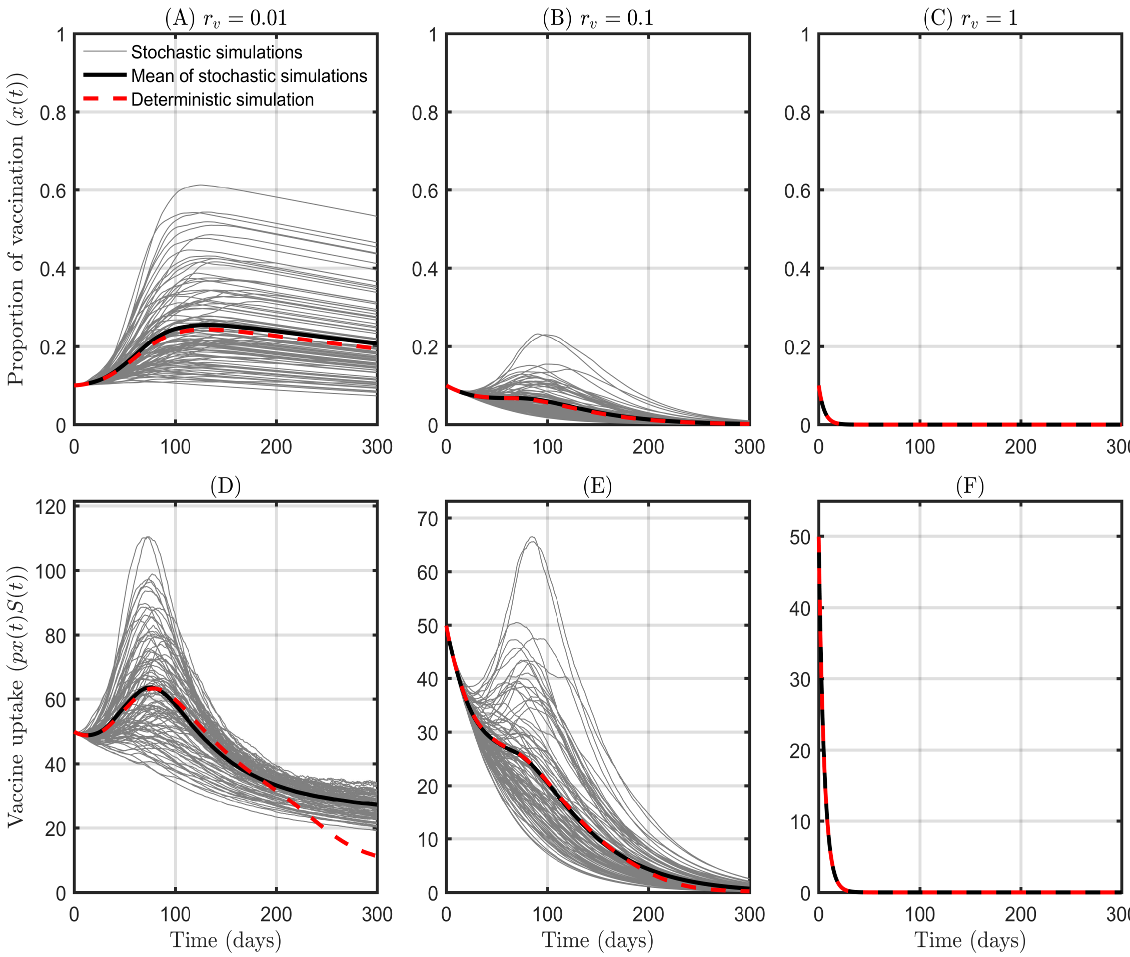


Figure C.14: The effect of perceived costs of vaccinators ($r_v$) on the proportion of vaccination and vaccine uptake under non-pharmaceutical interventions with moderately low mutation rates. Subfigures A, B, and C show the results of deterministic and 100 stochastic simulations of proportion of vaccination, when perceived costs of vaccinators are $r_v = 0.01$, $r_v = 0.1$, and $r_v = 1$, respectively. Subfigures D, E, and F show the change of vaccine uptake over time, for the same values of $r_v$ in the order specified above. Values of other parameters are $u_S = 1 \times 10^{-4}$, $u = 5 \times 10^{-5}$, $r_{A_{WT}} = 0.05$, and $r_{I_{WT}} = 0.06$.

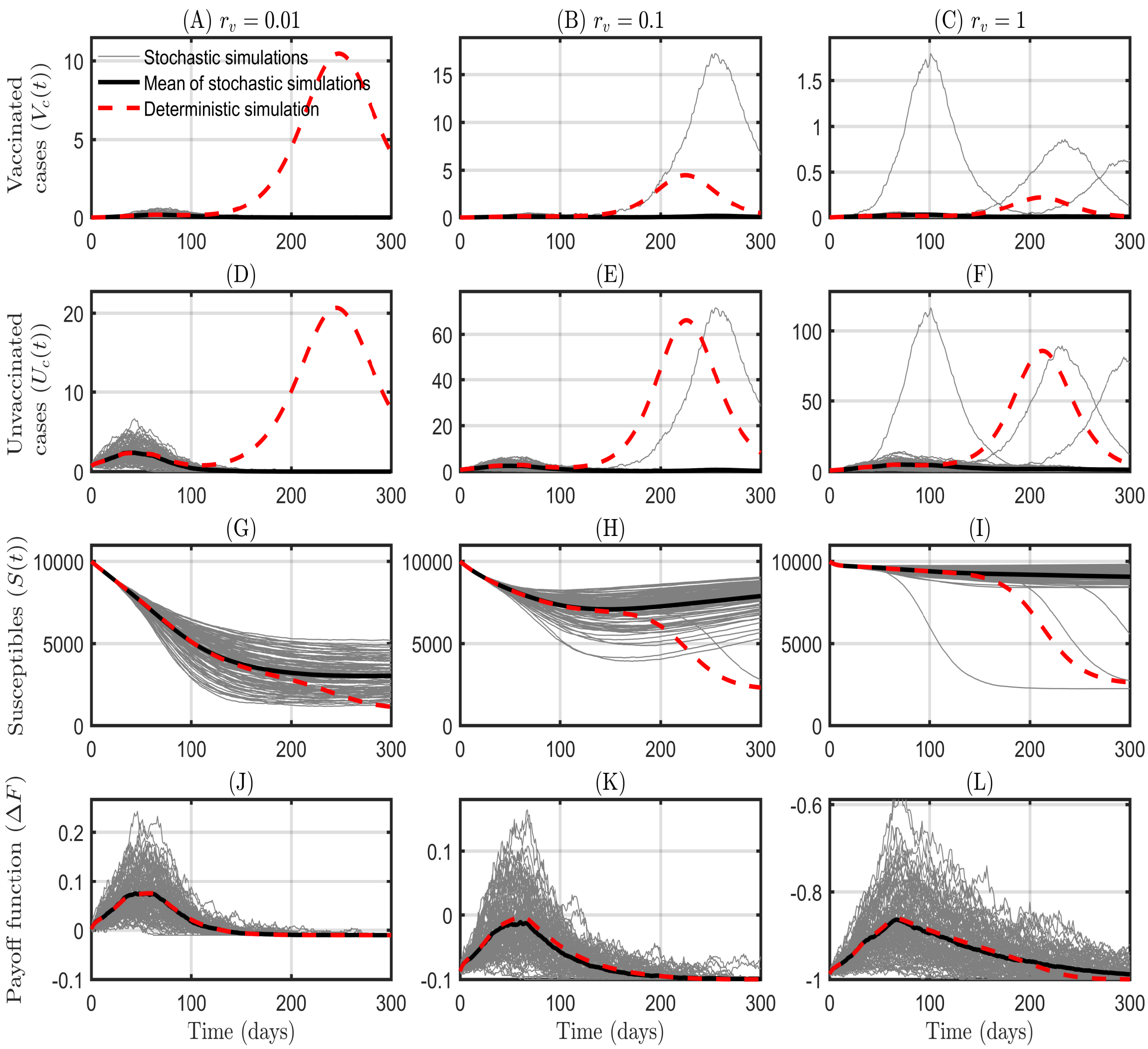


Figure C.15: The effect of perceived costs of vaccinators ($r_v$) on the vaccinated cases, unvaccinated cases, susceptibles, and payoff function under non-pharmaceutical interventions with moderately low mutation rates. Subfigures A, B, and C (D, E, and F) show the results of deterministic and 100 stochastic simulations of vaccinated (unvaccinated) cases, when perceived costs of vaccinators are $r_v = 0.01$, $r_v = 0.1$, and $r_v = 1$, respectively. Subfigures G, H, I, J, K, and L show the changes of susceptibles and payoff function over time, for the same values of $r_v$ in the order specified above. Values of other parameters are $u_S = 1 \times 10^{-4}$, $u = 5 \times 10^{-5}$, $r_{A_{WT}} = 0.05$, and $r_{I_{WT}} = 0.06$.

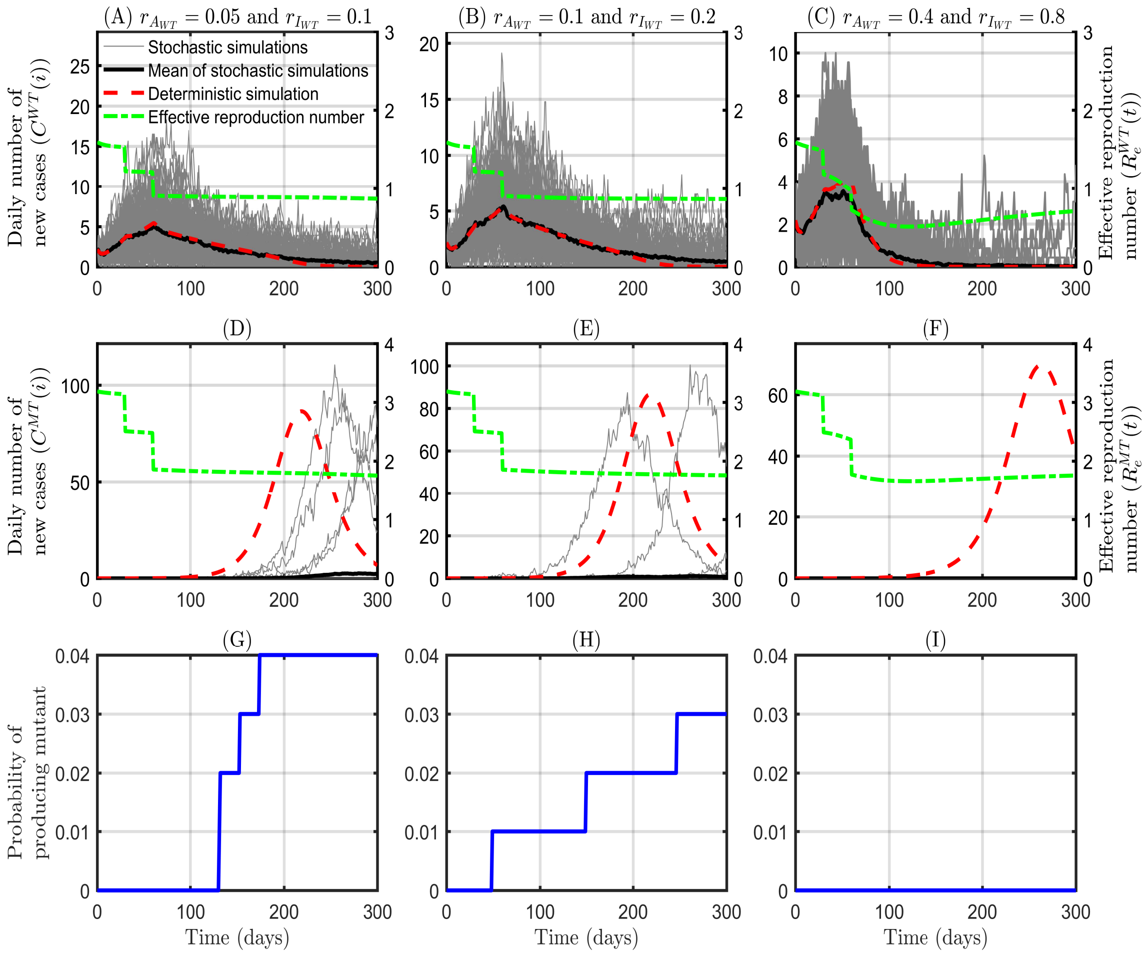


Figure C.16: The effect of perceived risks of WT infection ($r_{A_{WT}}$ and $r_{I_{WT}}$) on the probability of emergence of MT under non-pharmaceutical interventions with moderately low mutation rates. Subfigures A, B, and C (D, E, and F) show the results of deterministic and 100 stochastic simulations and the effective reproduction number of WT (MT), i.e. $R_e^{WT}(t)$ ($R_e^{MT}(t)$), when perceived risks of infection are $r_{A_{WT}} = 0.05$ and $r_{I_{WT}} = 0.1$; $r_{A_{WT}} = 0.1$ and $r_{I_{WT}} = 0.2$; and $r_{A_{WT}} = 0.4$ and $r_{I_{WT}} = 0.8$, respectively. Subfigures G, H, and I show the probability of producing a mutant strain over time, for the same sets of values of $r_{A_{WT}}$ and $r_{I_{WT}}$, in the order specified above. Values of other parameters are $u_S = 1 \times 10^{-4}$, $u_V = 5 \times 10^{-5}$, and $r_v = 0.6$.

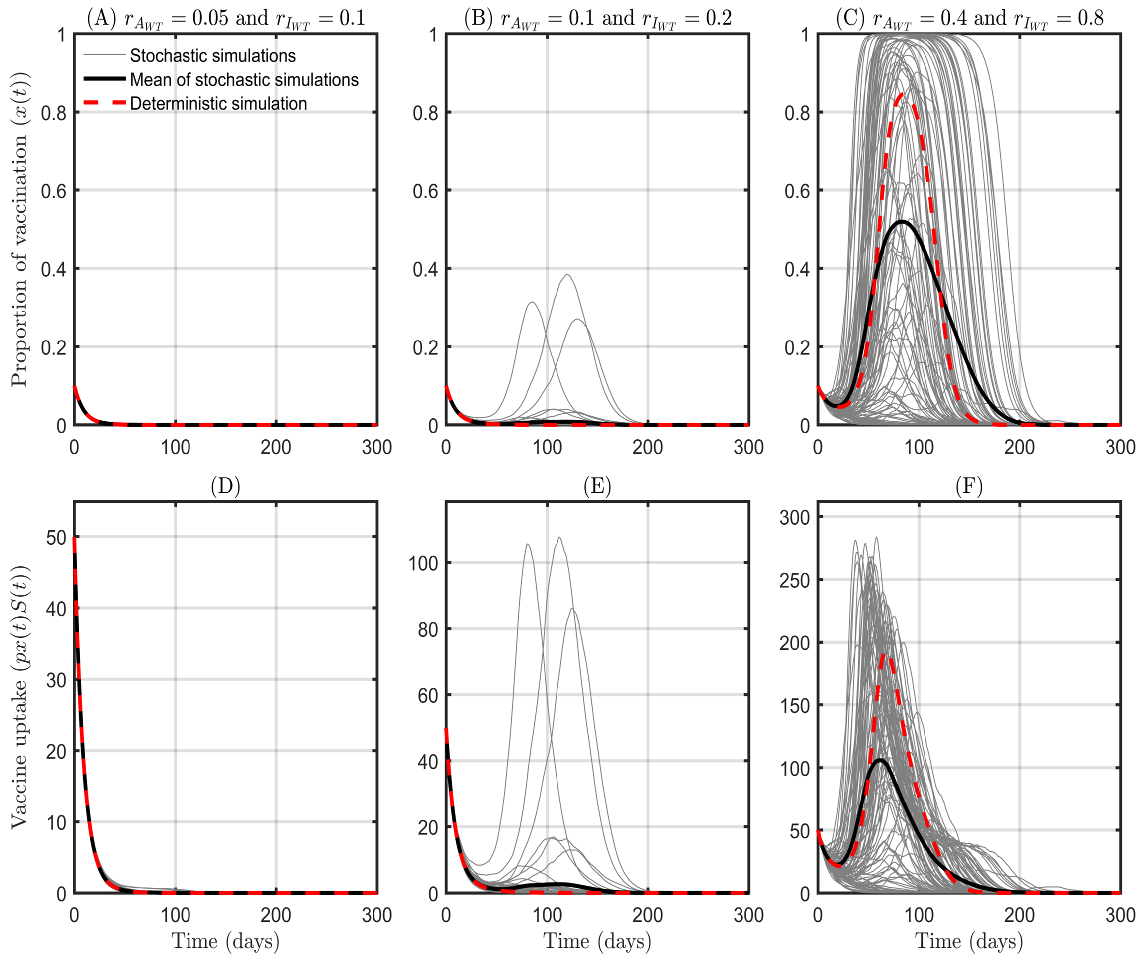


Figure C.17: The effect of perceived risks of WT infection ($r_{A_{WT}}$ and $r_{I_{WT}}$) on the proportion of vaccination and vaccine uptake under non-pharmaceutical interventions with moderately low mutation rates. Subfigures A, B, and C show the results of deterministic and 100 stochastic simulations of proportion of vaccination, when perceived risks of infection are $r_{A_{WT}} = 0.05$ and $r_{I_{WT}} = 0.1$; $r_{A_{WT}} = 0.1$ and $r_{I_{WT}} = 0.2$; and $r_{A_{WT}} = 0.4$ and $r_{I_{WT}} = 0.8$, respectively. Subfigures D, E, and F show the change of vaccine uptake over time, for the same sets of values of $r_{A_{WT}}$ and $r_{I_{WT}}$, in the order specified above. Values of other parameters are $u_S = 1 \times 10^{-4}$, $u_V = 5 \times 10^{-5}$, and $r_v = 0.6$.

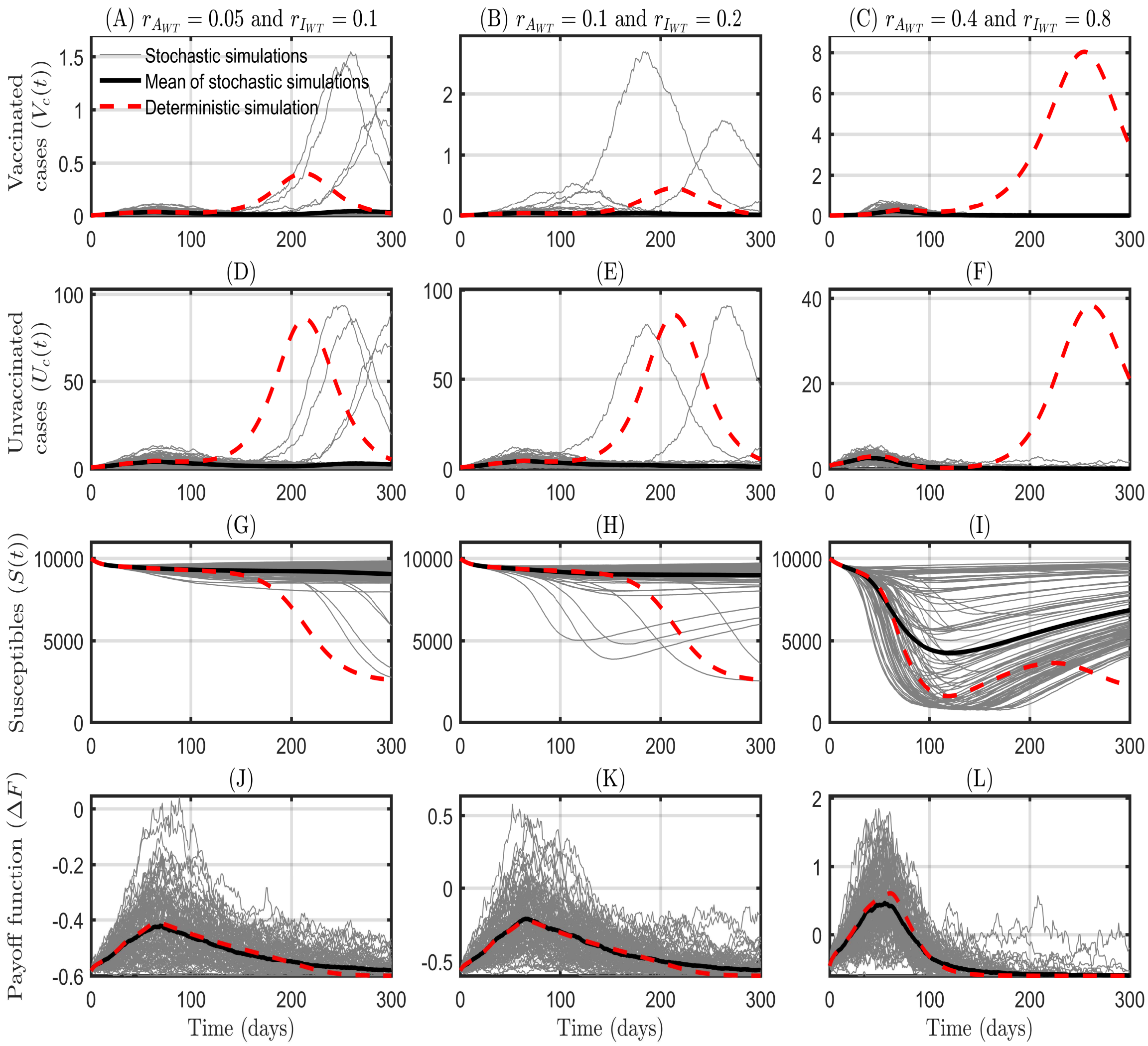


Figure C.18: The effect of perceived risks of WT infection ($r_{A_{WT}}$ and $r_{I_{WT}}$) on the vaccinated cases, unvaccinated cases, susceptibles, and payoff function under non-pharmaceutical interventions with moderately low mutation rates. Subfigures A, B, and C (D, E, and F) show the results of deterministic and 100 stochastic simulations of vaccinated (unvaccinated) cases, when perceived risks of infection are $r_{A_{WT}} = 0.05$ and $r_{I_{WT}} = 0.1$; $r_{A_{WT}} = 0.1$ and $r_{I_{WT}} = 0.2$; and $r_{A_{WT}} = 0.4$ and $r_{I_{WT}} = 0.8$, respectively. Subfigures G, H, I, J, K, and L show the changes of susceptibles and payoff function over time, for the same sets of values of $r_{A_{WT}}$ and $r_{I_{WT}}$, in the order specified above. Values of other parameters are $u_S = 1 \times 10^{-4}$, $u_V = 5 \times 10^{-5}$, and $r_v = 0.6$.

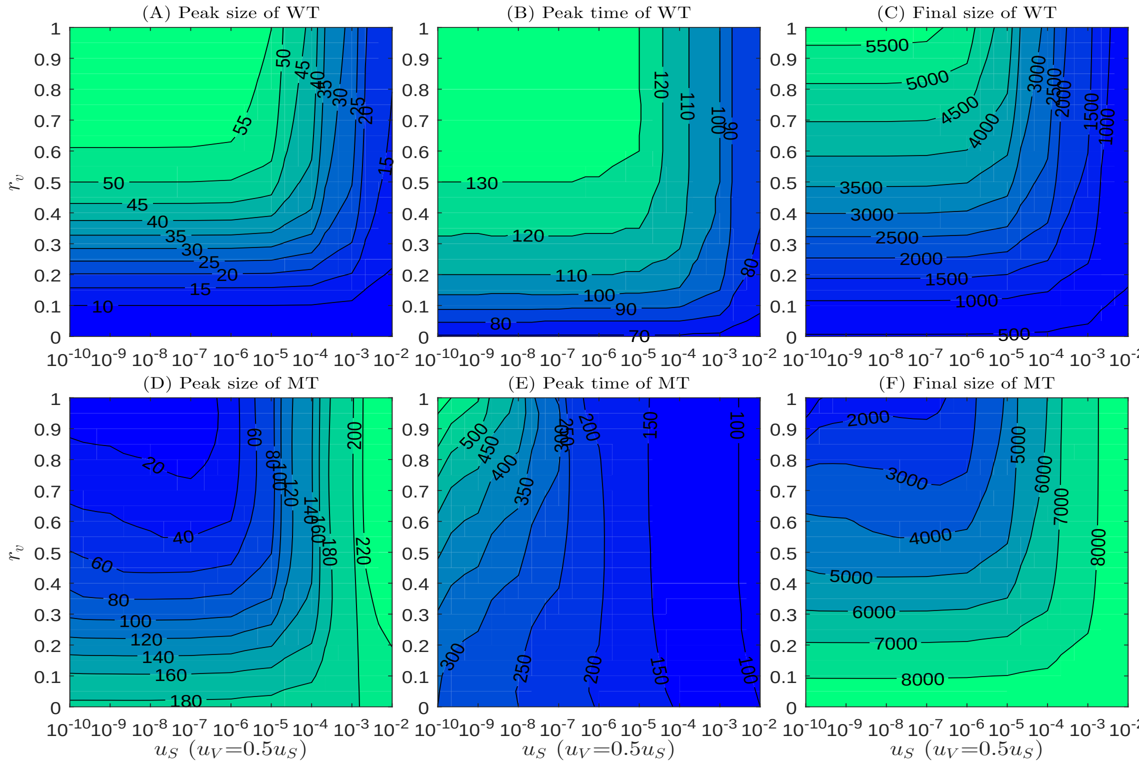


Figure C.19: Impact of perceived costs of vaccinators and mutation probability on peak size, peak time, and final outbreak size for $r_{A_{WT}} = r_{A_{MT}} = 0.05$ and $r_{I_{WT}} = r_{I_{MT}} = 0.1$. Subfigures A, B, and C (D, E, and F) show the peak number of daily infections, day when peak occurs, and total number of infections for WT (MT).

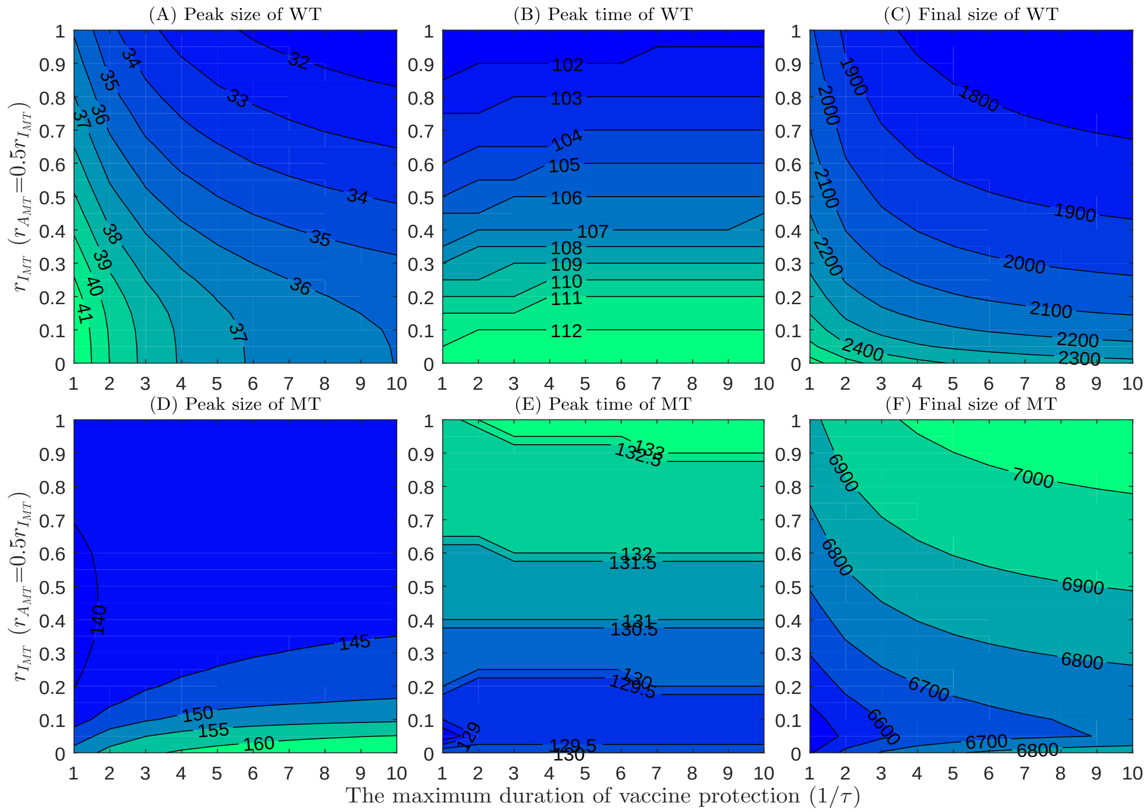


Figure C.20: Impact of perceived risks of MT infection and the maximum duration of vaccine protection on peak size, peak time, and final outbreak size for $r_{A_{WT}} = 0.05$, $r_{I_{WT}} = 0.1$, $r_v = 0.6$, $u_S = 2 \times 10^{-4}$, and $u_V = 1 \times 10^{-4}$. Subfigures A, B, and C (D, E, and F) show the peak number of daily infections, day when peak occurs, and total number of infections for WT (MT).

# References

[1] C. N. Ngonghala, P. Goel, D. Kutor, S. Bhattacharyya, Human choice to self-isolate in the face of the COVID-19 pandemic: a game dynamic modelling approach, Journal of Theoretical Biology 521 (2021) 110692.

[2] P. Van den Driessche, J. Watmough, Reproduction numbers and sub-threshold endemic equilibria for compartmental models of disease transmission, Mathematical Biosciences 180 (1-2) (2002) 29–48.

[3] O. Diekmann, J. A. P. Heesterbeek, J. A. Metz, On the definition and the computation of the basic reproduction ratio r0 in models for infectious diseases in heterogeneous populations, Journal of Mathematical Biology 28 (4) (1990) 365–382.